

Supporting Information for:

**H-atom abstraction reaction for organic substrates *via*
mononuclear copper(II)-superoxo species as a model of D β M and
PHM**

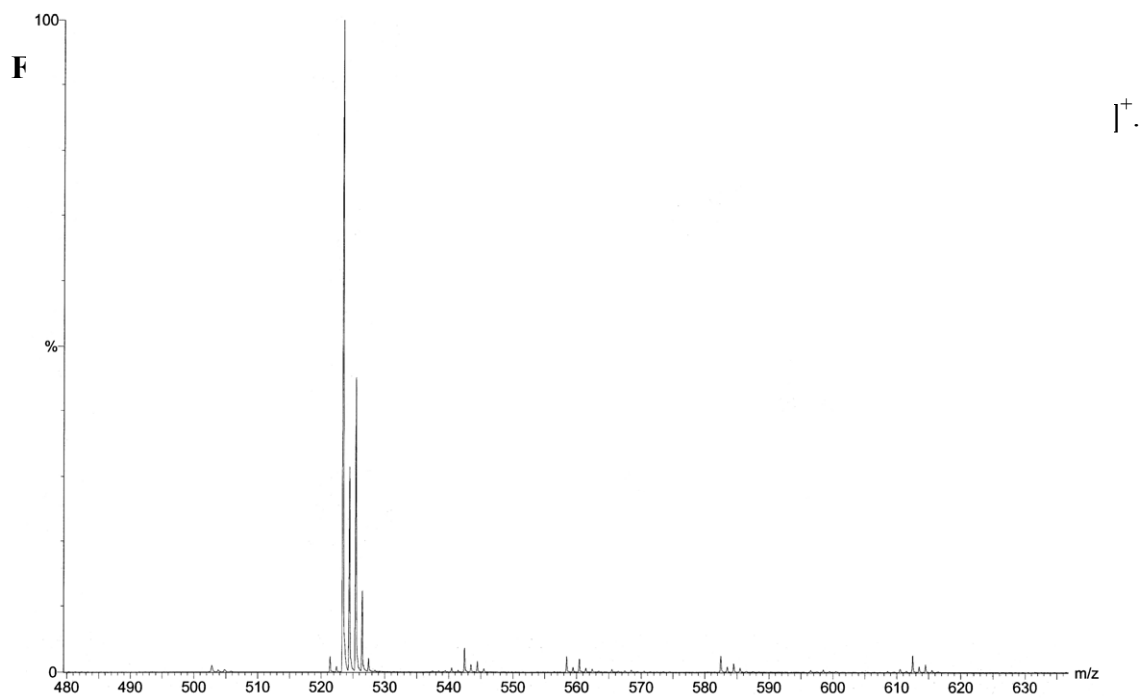
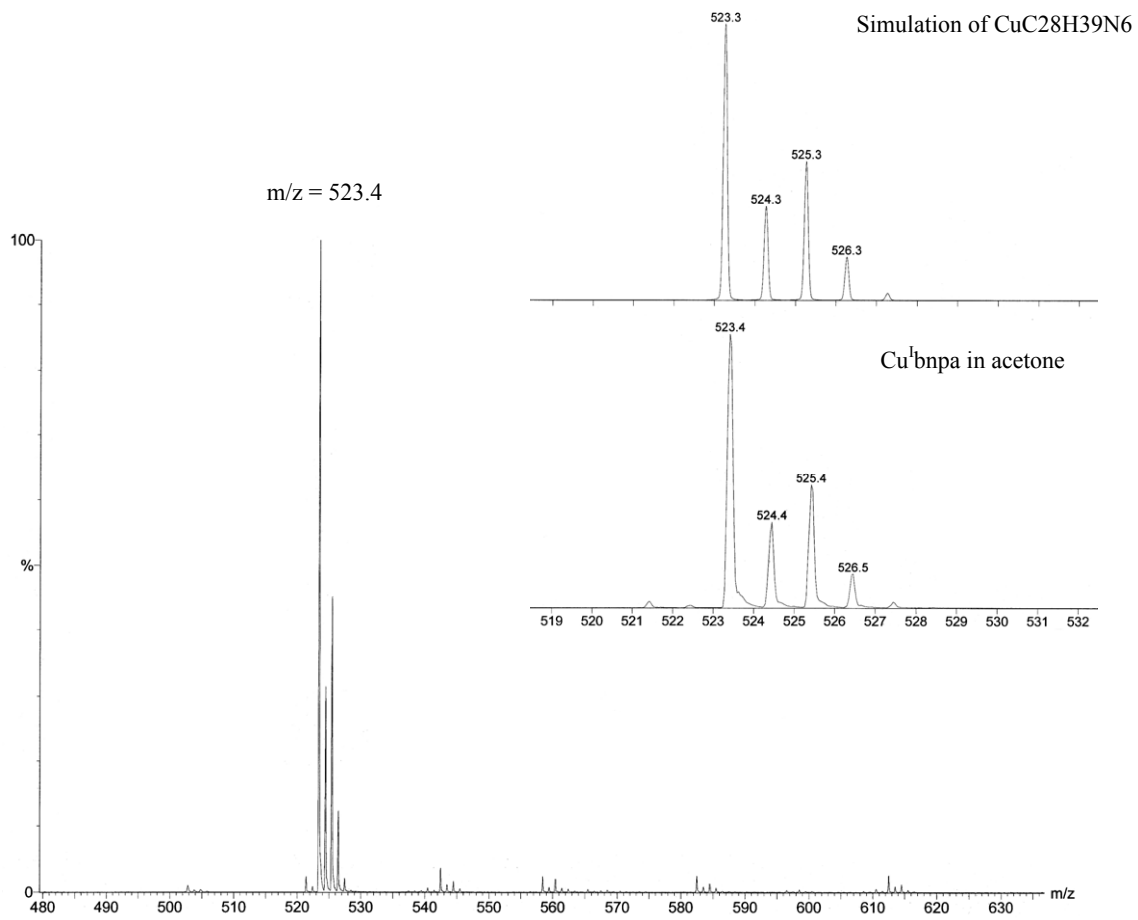
Tatsuya Fujii,^a Syuhei Yamaguchi^a Shun Hirota^b and Hideki Masuda^{a*}

^aDepartment of Applied Chemistry, Nagoya Institute of Technology, Showa-ku, Nagoya 466-8555, Japan. Fax: +81-52-735-5209; Tel: +81-52-735-5228; *E-mail: masuda.hideki@nitech.ac.jp

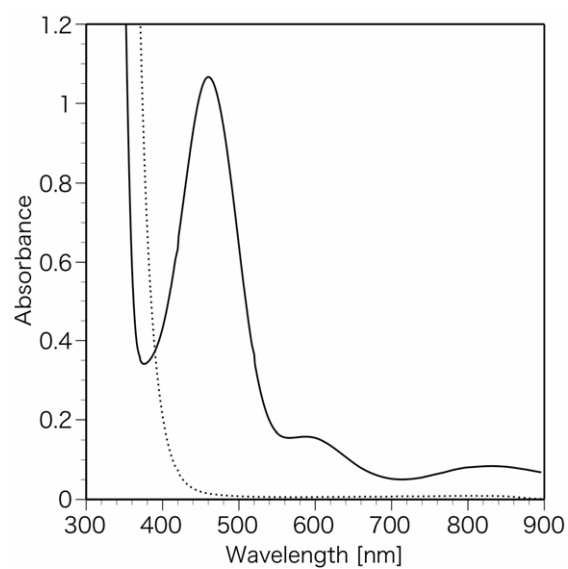
^b Graduate School of Material Science, Nara Institute of Science and Technology.

Contents:

- 1) The ESI-mass spectrum of complex **1**. **Fig. S1**
- 2) UV-vis spectra of the reaction of **1** with O₂. **Fig. S2**
- 3) Concentration dependence of the decomposition rate of **2**. **Fig. S3**
- 4) Calculation of the generation rate of **2**. **Fig. S4**
- 5) UV-vis spectra of the reaction of **2** with DMPO. **Fig. S5**
- 6) ESI-mass spectrum of the reaction of **1** with O₂ in the presence of DMPO. **Fig. S6**
- 7) Spectroscopic feature of the [Cu^{II}(bnpa)(OOH)]⁺ complex. **Fig. S7**
- 8) UV-vis spectra of the reaction of **2** with TMPO-H. **Fig. S8**
- 9) ESI-mass spectrum of the reaction of **1** with O₂ in the presence of TEMPO-H. **Fig. S9**
- 10) UV-vis spectral change of the reaction of **1** with O₂ in the presence of phenylhydrazine. **Fig. S10**
- 11) ESI-mass spectrum of the reaction of **1** with O₂ in the presence of phenylhydrazine. **Fig. S11**



(a) MeOH solution



(b) THF solution

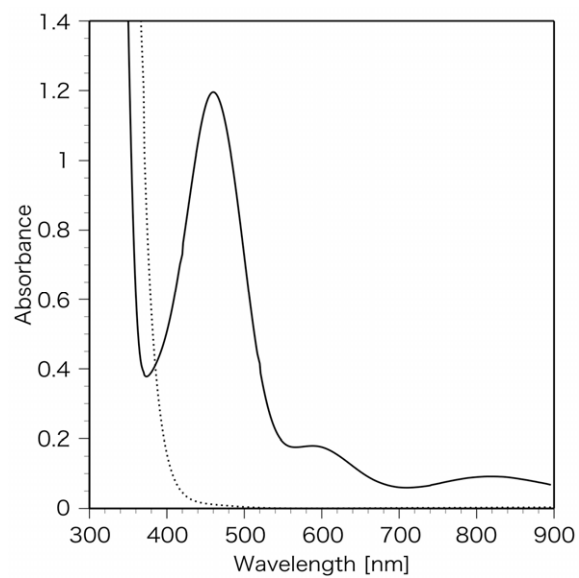


Fig.S2 UV-vis spectral change of the reaction of **1** (0.5 mM) with O₂ in MeOH and THF solutions at -80 °C.

List of the characteristic LMCT band after bubbling O₂

(a) 460 nm ($\epsilon = 4270 \text{ M}^{-1}\text{cm}^{-1}$), 580 nm ($\epsilon = 630 \text{ M}^{-1}\text{cm}^{-1}$)

(b) 460 nm ($\epsilon = 4780 \text{ M}^{-1}\text{cm}^{-1}$), 580 nm ($\epsilon = 720 \text{ M}^{-1}\text{cm}^{-1}$)

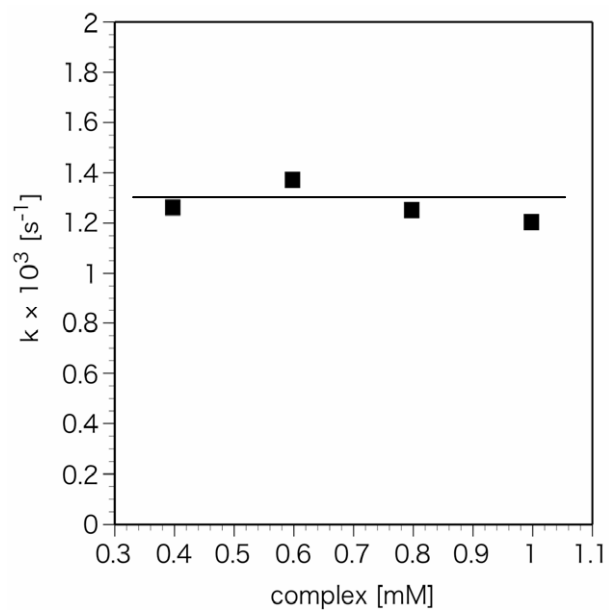


Fig.S3 Plots of decomposition rates (k) vs. concentrations of **1** in acetone at $-20\text{ }^\circ\text{C}$.

Decomposition process obeyed first-order kinetics.

$$k_1 = 1.26 \times 10^{-3} \text{ s}^{-1} : \text{complex } 0.4 \text{ mM}$$

$$k_2 = 1.37 \times 10^{-3} \text{ s}^{-1} : \text{complex } 0.6 \text{ mM}$$

$$k_3 = 1.25 \times 10^{-3} \text{ s}^{-1} : \text{complex } 0.8 \text{ mM}$$

$$k_4 = 1.20 \times 10^{-3} \text{ s}^{-1} : \text{complex } 1.0 \text{ mM}$$

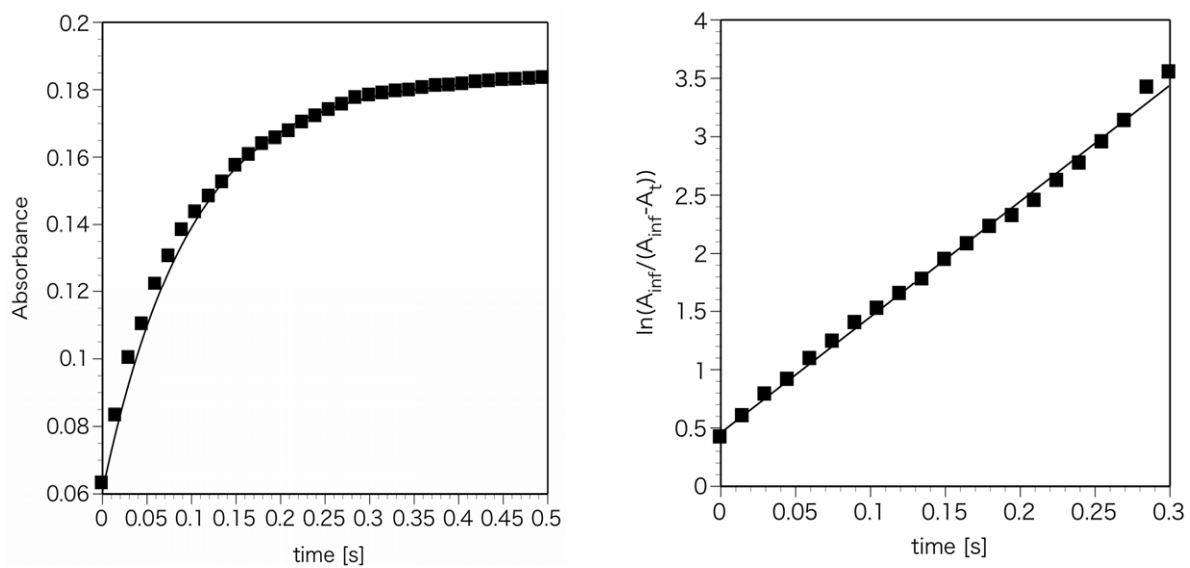


Fig.S4 Estimation of the generation rate for the $[\text{Cu}^{\text{II}}(\text{bnpa})(\text{O}_2^{2-})]^{2+}$ (**2**) in acetone (0.25 mM) at 10 °C. Time course of the absorption change at 460 nm and it's first-order fitting.

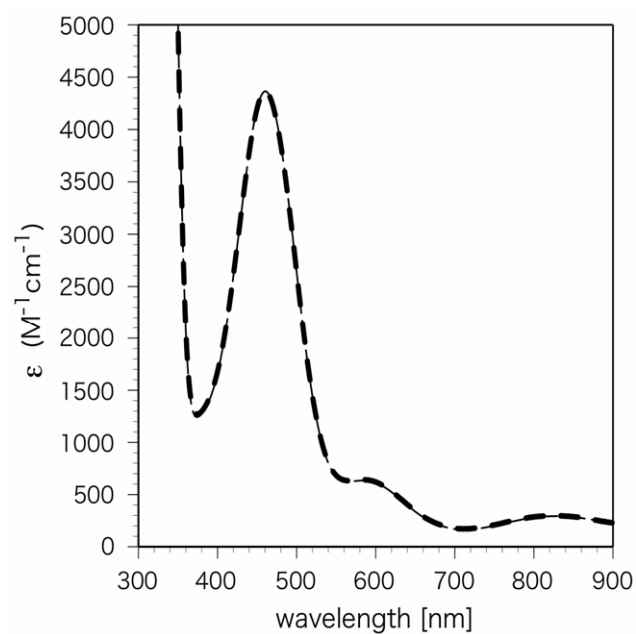


Fig.S5 UV-vis spectral change of the reaction of **2** (0.5 mM) with DMPO (50 mM) in acetone solution at -80 °C.

(a) solid line : Spectrum of the $[Cu^{II}(bnpa)(O_2^{2-})]^{2+}$ (**2**) after bubbling Ar gas.

(b) dotted line : Spectrum of the solution after adding DMPO.

* Reversibility was not observed by bubbling Ar gas in the solution of **2**.

* Spectral change was not observed by adding DMPO.

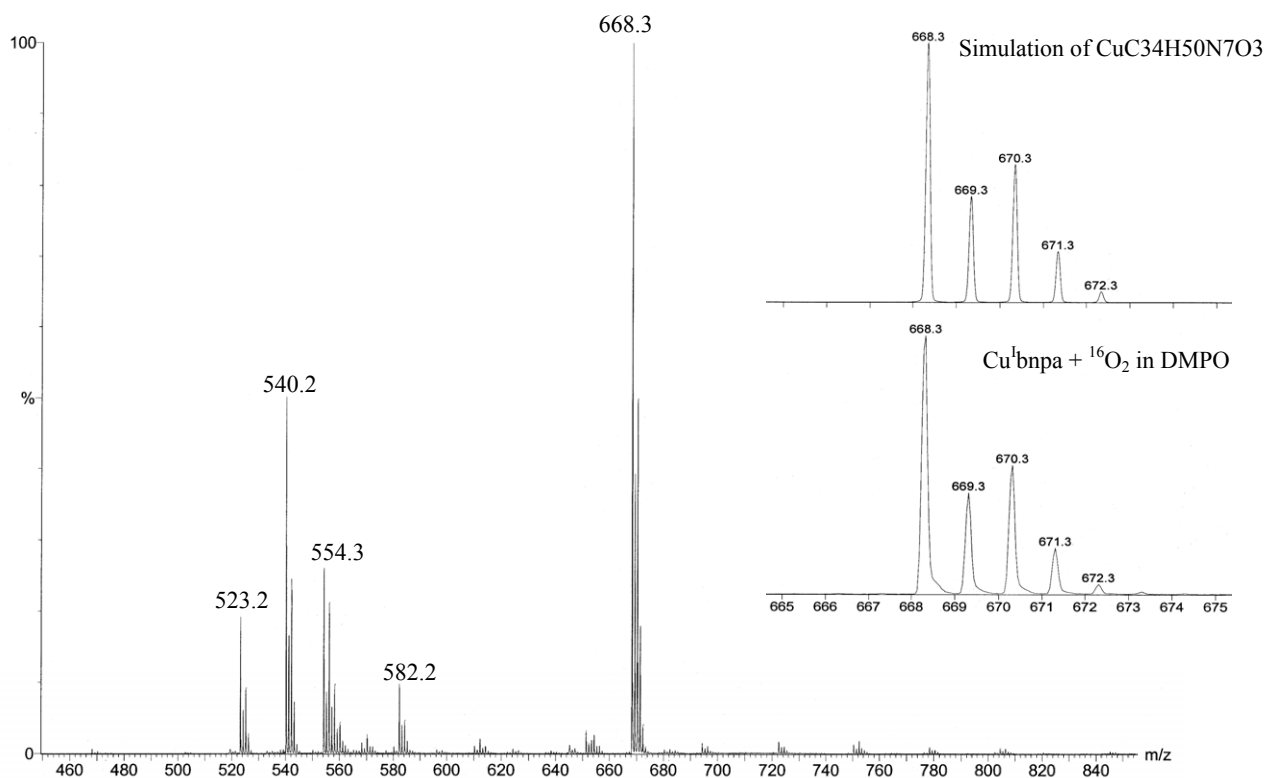


Fig.S6(a) ESI-mass spectra of the reaction solution of **1** with $^{16}\text{O}_2$ in the presence of a large excess amount of DMPO in acetone. (inset) Comparison of the parent peak and isotope simulation of $[\text{Cu}^{\text{II}}(\text{bnpa})(^{16}\text{O}_2^-)(\text{DMPO})]^+$.

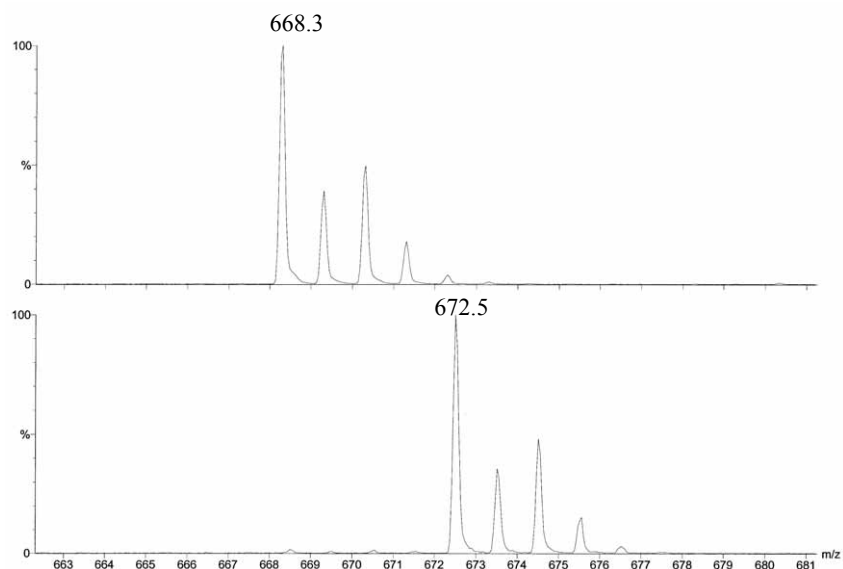


Fig.S6(b) Comparison of the ESI-mass spectra for the reaction solution of **1** with $^{16}\text{O}_2$ and $^{18}\text{O}_2$ in the presence of a large excess amount of DMPO in acetone. (top) **1** + $^{16}\text{O}_2$, (bottom) **1** + $^{18}\text{O}_2$

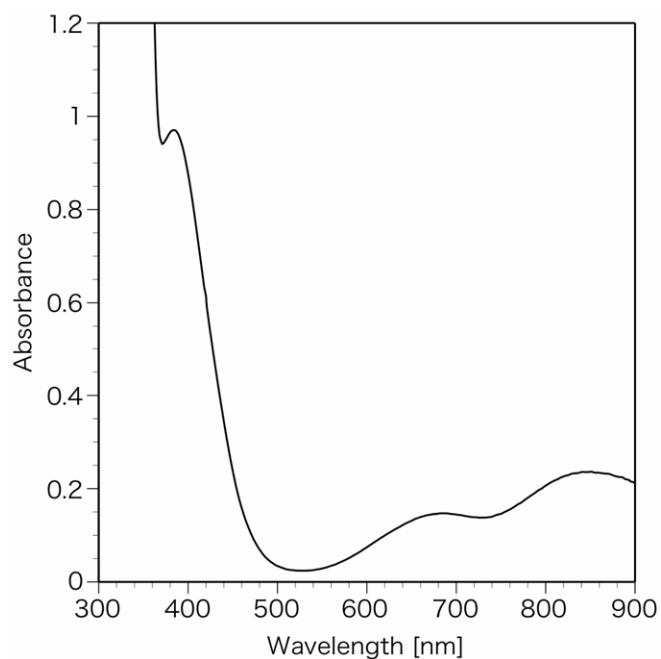


Fig.S7 UV-vis spectrum of $[\text{Cu}^{\text{II}}(\text{bnpa})(\text{OOH})]^+$ (1 mM) prepared by the reaction of $[\text{Cu}^{\text{II}}(\text{bnpa})]^+$ with H_2O_2 (10eq) in acetone solution at $-40\text{ }^\circ\text{C}$.

380 nm ($\epsilon = 970\text{ M}^{-1}\text{cm}^{-1}$) : LMCT band ($\text{OOH} \rightarrow \text{Cu}^{\text{II}}$)

680 nm ($\epsilon = 147\text{ M}^{-1}\text{cm}^{-1}$), 840 nm ($\epsilon = 235\text{ M}^{-1}\text{cm}^{-1}$) : d-d band

* The formation of $[\text{Cu}^{\text{II}}(\text{bnpa})(\text{OOH})]^+$ was also confirmed from other spectroscopic measurements (ESI-mass, ESR, rRaman).¹⁸

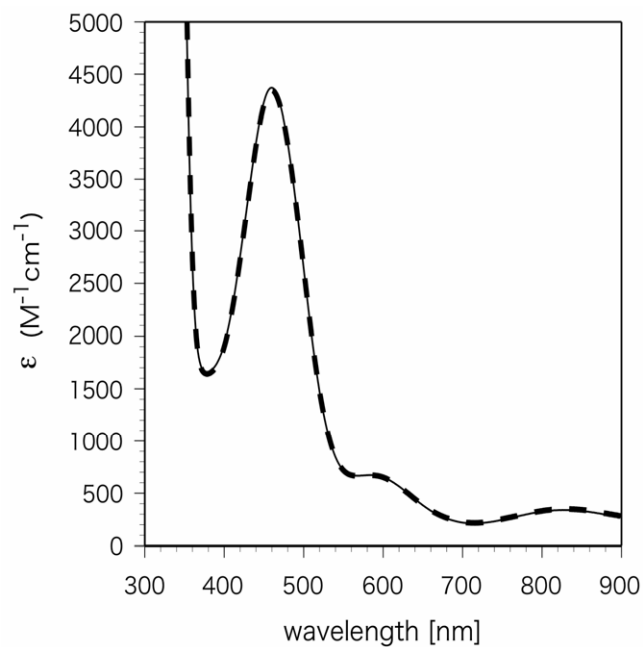


Fig.S8 UV-vis spectral change of the reaction of **2** (0.5 mM) with TEMPO-H (50 mM) in acetone solution at -80 °C.

- (a) solid line : Spectrum of the $[Cu^{II}(bnpa)(O_2^{2-})]^{2+}$ (**2**) after bubbling Ar gas.
(b) dotted line : Spectrum of the solution after adding TEMPO-H.

* Spectral change was not observed by adding TEMPO-H.

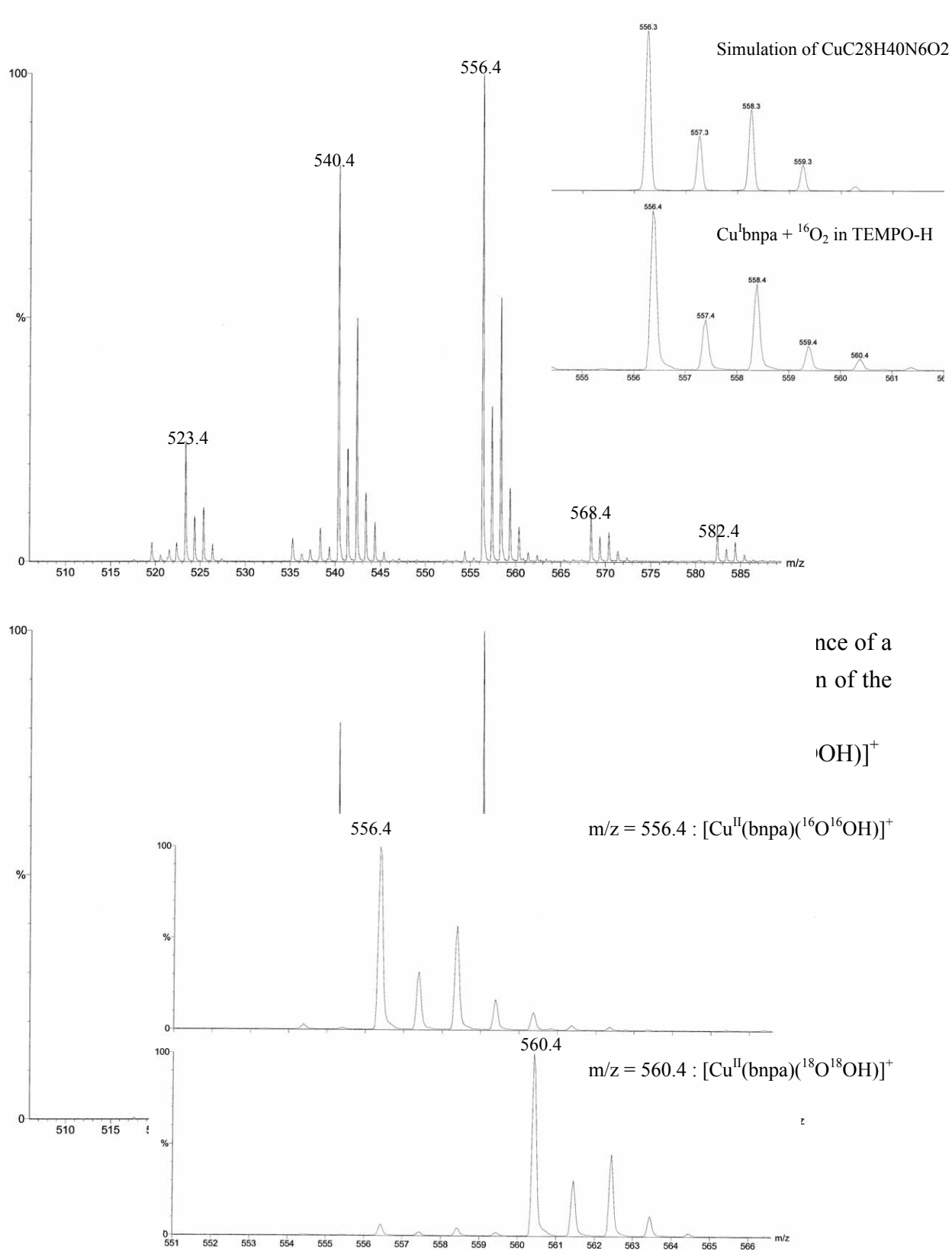


Fig.S9(b) Comparison of the ESI-mass spectra for the reaction solution of **1** with ${}^{16}\text{O}_2$ and ${}^{18}\text{O}_2$ in the presence of a large excess amount of TEMPO-H in acetone. (top) **1** + ${}^{16}\text{O}_2$, (bottom) **1** + ${}^{18}\text{O}_2$

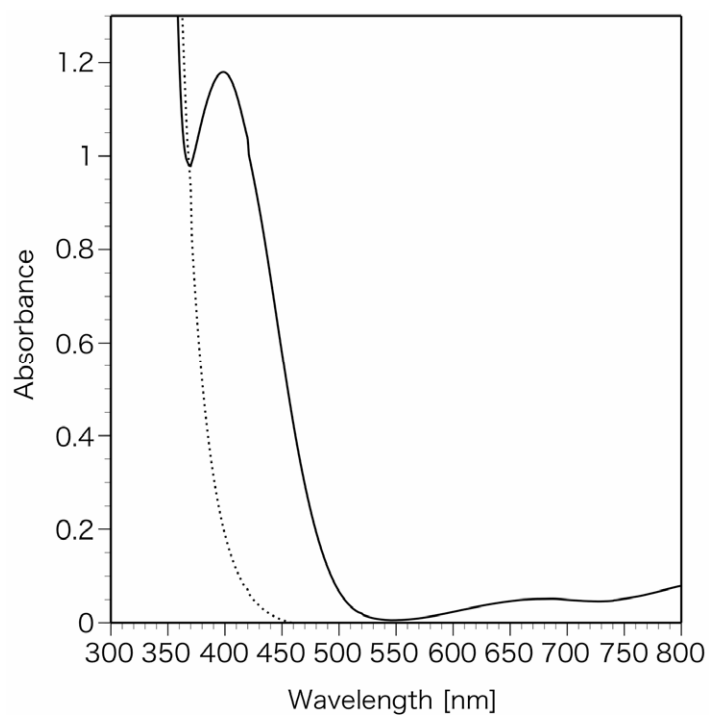


Fig.S10 UV-vis spectral change in the reaction of **1** with O₂ in the presence of a large excess amount of phenylhydrazine in acetone at -80 °C.
(dotted line) complex **1** (0.5 mM) + phenylhydrazine (100 eq)
(solid line) after O₂ bubbling

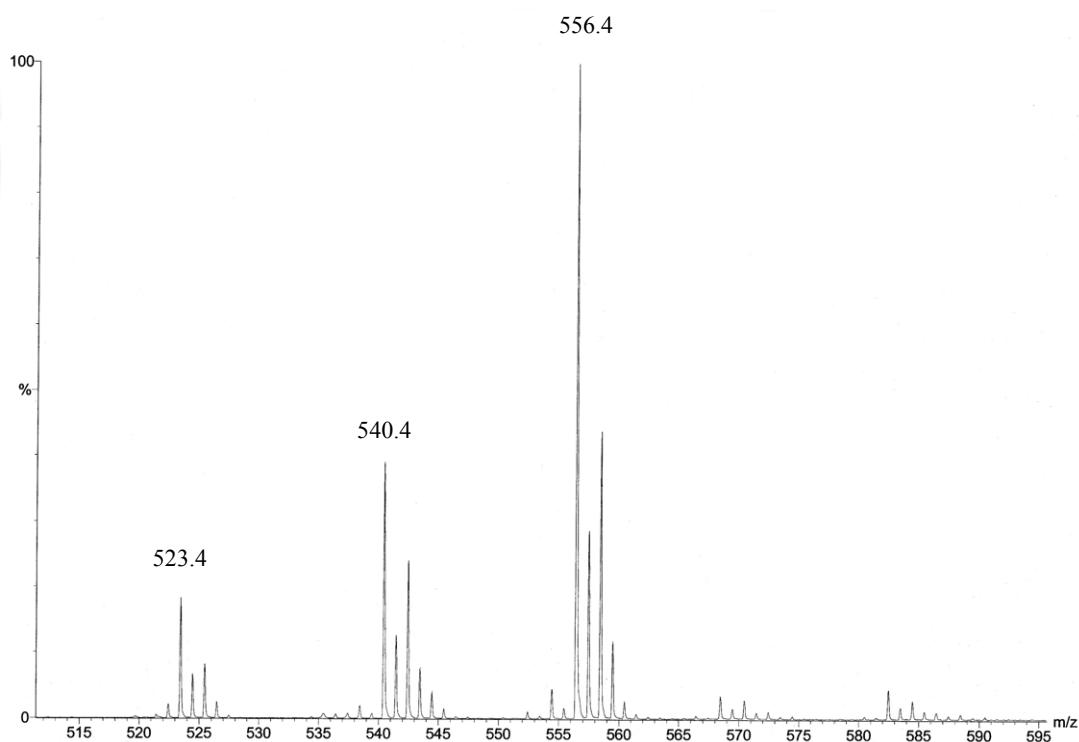


Fig.S11(a) ESI-mass spectra of the reaction solution of **1** with $^{16}\text{O}_2$ in the presence of a large amount of phenylhydrazine in acetone.

$m/z = 523.4 : [\text{Cu}^{\text{I}}(\text{bnpa})]^+$, $540.4 : [\text{Cu}^{\text{II}}(\text{bnpa})(\text{OH})]^+$, $556.4 : [\text{Cu}^{\text{II}}(\text{bnpa})(^{16}\text{O}^{16}\text{OH})]^+$

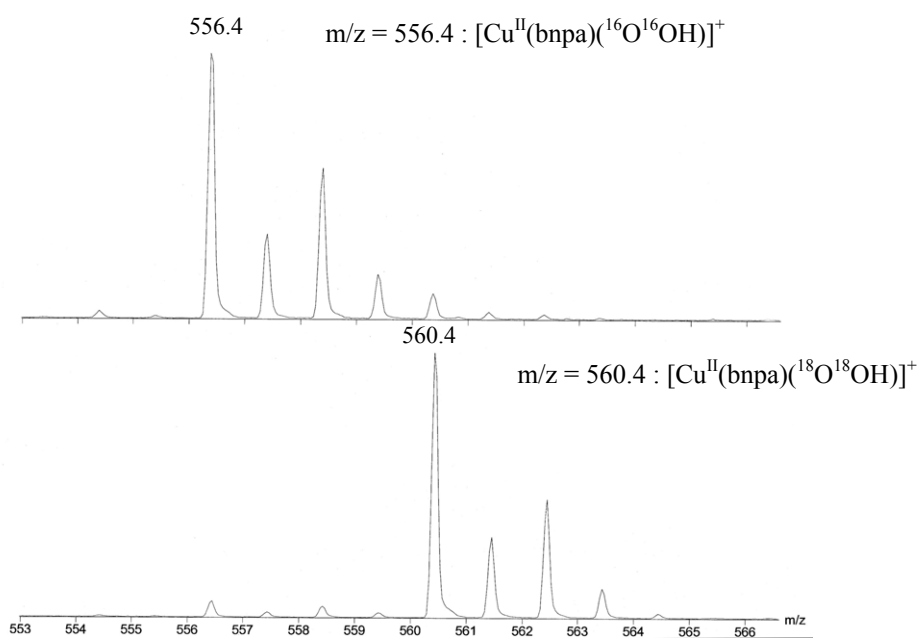


Fig.S11(b) Comparison of the ESI-mass spectra for the reaction solution of **1** with $^{16}\text{O}_2$ and $^{18}\text{O}_2$ in the presence of a large amount of Phenylhydrazine in acetone. (top) **1** + $^{16}\text{O}_2$, (bottom) **1** + $^{18}\text{O}_2$